

A subcortical pathway to the right amygdala mediating "unseen" fear

J. S. Morris, A. Öhman, and R. J. Dolan

PNAS 1999;96:1680-1685

doi:10.1073/pnas.96.4.1680

This information is current as of October 2006.

Online Information & Services	High-resolution figures, a citation map, links to PubMed and Google Scholar, etc., can be found at: www.pnas.org/cgi/content/full/96/4/1680
References	This article cites 46 articles, 18 of which you can access for free at: www.pnas.org/cgi/content/full/96/4/1680#BIBL This article has been cited by other articles: www.pnas.org/cgi/content/full/96/4/1680#otherarticles
E-mail Alerts	Receive free email alerts when new articles cite this article - sign up in the box at the top right corner of the article or click here .
Rights & Permissions	To reproduce this article in part (figures, tables) or in entirety, see: www.pnas.org/misc/rightperm.shtml
Reprints	To order reprints, see: www.pnas.org/misc/reprints.shtml

Notes:

A subcortical pathway to the right amygdala mediating “unseen” fear

J. S. MORRIS*, A. ÖHMAN†, AND R. J. DOLAN*‡§

*Wellcome Department of Cognitive Neurology, Queen Square, London, WC1N 3BG, United Kingdom; †Department of Clinical Neuroscience, Section of Psychiatry and Psychology, Karolinska Hospital, S-17176 Stockholm, Sweden; and ‡Royal Free and University College Hospitals School of Medicine, Rowland Hill Street, London NW3 2DF, United Kingdom

Communicated by Lawrence Weiskrantz, University of Oxford, Oxford, United Kingdom, December 9, 1998 (received for review October 20, 1998)

ABSTRACT Neuroimaging studies have shown differential amygdala responses to masked (“unseen”) emotional stimuli. How visual signals related to such unseen stimuli access the amygdala is unknown. A possible pathway, involving the superior colliculus and pulvinar, is suggested by observations of patients with striate cortex lesions who show preserved abilities to localize and discriminate visual stimuli that are not consciously perceived (“blindsight”). We used measures of right amygdala neural activity acquired from volunteer subjects viewing masked fear-conditioned faces to determine whether a colliculo-pulvinar pathway was engaged during processing of these unseen target stimuli. Increased connectivity between right amygdala, pulvinar, and superior colliculus was evident when fear-conditioned faces were unseen rather than seen. Right amygdala connectivity with fusiform and orbitofrontal cortices decreased in the same condition. By contrast, the left amygdala, whose activity did not discriminate seen and unseen fear-conditioned targets, showed no masking-dependent changes in connectivity with superior colliculus or pulvinar. These results suggest that a subcortical pathway to the right amygdala, via midbrain and thalamus, provides a route for processing behaviorally relevant unseen visual events in parallel to a cortical route necessary for conscious identification.

Conscious awareness of a brief (<40 ms) visual target can be prevented by the use of a suitable masking stimulus. If the target stimulus has been aversively conditioned, however, it can elicit reliable skin-conductance responses even when masked and therefore “unseen” (1). The amygdaloid complex in the medial temporal lobe has been implicated in lesion studies in the mediation of aversive (or “fear”) conditioning (2, 3) and the processing of other fear-related stimuli (4, 5). Functional neuroimaging experiments have demonstrated differential amygdala responses to both seen (6, 7) and unseen (8, 9) fear-related stimuli. Although the amygdala is known to receive a large visual input from the anterior temporal lobe (10), the neural pathways by which masked stimuli reach the amygdala have not been previously investigated.

Studies of patients with lesions to striate cortex have provided evidence for parallel visual systems in the brain associated with different levels of conscious awareness. Despite having no conscious perception of stimuli in their blind fields, patients with striate cortex lesions can nevertheless exhibit residual visual abilities or “blindsight” by accurately guessing the location of visual targets (11–14). One hypothesis regarding the neural basis of blindsight is that the preserved abilities of patients are mediated by a parallel secondary visual pathway comprising the superior colliculus in the midbrain tectum and the pulvinar nucleus in the posterior thalamus (11, 15–17). This

proposal has received support from behavioral and functional neuroimaging studies of patients with selective brain lesions (16, 18–22). We conjectured, given the existence of a strong pulvinar-amygdala projection in primates (23), that the same structures implicated in mediating blindsight (i.e., superior colliculus and pulvinar) also contribute to amygdala processing of masked stimuli.

To address the question of amygdala connectivity during unconscious processing of behaviorally relevant stimuli, we conducted a further analysis of previously reported neuroimaging data in which enhanced right amygdala activity was recorded during the presentation of masked conditioned faces (9). By using these data, we examined how right amygdala responses covaried with activity in other brain regions under different experimental conditions. Brain areas constituting a functionally cooperative network in a particular psychological condition can be expected to show increased covariation of activity specific to that context. Therefore, to identify structures with increased connectivity to the right amygdala during unconscious processing, we directly compared, at every brain voxel, the covariation of responses during presentation of the masked conditioned faces with the covariation in all other experimental conditions (24).

METHODS

Subjects. Ten healthy, right-handed male subjects (mean age 32.7 years) participated in the study. They all gave informed consent to the experiment, which was approved by the local hospital ethics committee and Administration of Radioactive Substances Advisory Committee (U.K.).

Positron-Emission Tomography (PET) Scan Acquisition. Subjects had 12 scans of the distribution of $H_2^{15}O$ acquired with a Siemens/CPS ECAT EXACT HR⁺ PET scanner (Siemens/CTI, Knoxville, TN) operated in high-sensitivity three-dimensional mode. Subjects received a total of 350 MBq of $H_2^{15}O$ intravenously over 20 seconds. A Hanning filter was used to reconstruct the images into 63 planes, resulting in a 6.4-mm transaxial and 5.7-mm axial resolution (full width half maximum).

Statistical Analysis. After realignment, scans were transformed into a standard stereotactic space (25, 26). Structural MRIs from each subject were coregistered into the same space. A Gaussian filter set at 12 mm full width at half maximum was used to smooth the PET data, which were adjusted to a global mean of 50 ml/dl·min⁻¹. A blocked (by subject) analysis of covariance (ANCOVA) model was fitted to the data at each voxel with condition effects for each of the four experimental conditions and global cerebral blood flow (CBF) as a confounding covariate. Contrasts of the condition

The publication costs of this article were defrayed in part by page charge payment. This article must therefore be hereby marked “advertisement” in accordance with 18 U.S.C. §1734 solely to indicate this fact.

PNAS is available online at www.pnas.org.

Abbreviations: PET, positron-emission tomography; CS, conditioned stimulus; SPM, statistical parametric mapping; CBF, cerebral blood flow.

§To whom reprint requests should be addressed. e-mail: r.dolan@fil.ion.ucl.ac.uk.

effects at each voxel were assessed by using a *t* statistic. *P* values for activations in the amygdala were corrected for the volume of brain analyzed, specified as a sphere with radius 8 mm (27). *P* values for other activations were corrected for multiple nonindependent comparisons (27). In all cases, localization of the group mean activations was confirmed by registration with subjects' own MRIs. The PET data were analyzed by using statistical parametric mapping (SPM96) software from the Wellcome Department of Cognitive Neurology (London).

In the regression analysis, adjusted regional cerebral blood flow values at the maximal focus of activation in the right amygdala, ($x = 18, y = -2, z = -28$), were grouped into the four experimental conditions. These values were then used as covariates of interest in a separate analysis to test for psychophysiological interactions or context-specific changes in covariance (24). The condition blocks and ungrouped right amygdala CBF values were used as confounding covariates. Differences between the regression slopes obtained for the covariates of interest were tested directly for every voxel in the brain to produce a SPM(*t*) showing voxels in which covariance of activity with the right amygdala changed significantly as a function of experimental condition.

Experimental Design. In an initial conditioning phase immediately preceding scanning, subjects viewed a sequence of grayscale images of faces presented singly on a computer monitor screen for 75 ms at intervals of 15–25 s (mean 20 s). Four faces taken from a standard set of pictures of facial affect were used—two with angry expressions and two with neutral expressions. Each face was shown six times in a pseudorandom order. One of the angry faces (the CS+) was always followed by a 1-s 100-dB white noise burst. The identity of the CS+ face was balanced across subjects. None of the other faces was ever paired with the noise. Before each of the 12 scanning windows, which occurred at 8-min intervals, a shortened conditioning sequence was played consisting of three repetitions of the four faces. During the 90-s scanning window that seamlessly followed the conditioning phase, 12 pairs of faces, consisting of a target and a mask, were shown at 5-s intervals. The target face was presented for 30 ms and immediately followed by the masking face for 45 ms (Fig. 1c).

There were four different conditions: (i) unseen CS+, in which the CS+ (noise-paired) angry face was the target and a neutral face was the mask; (ii) seen CS+, in which a neutral face was the target and the CS+ face was the (perceived) mask; (iii) unseen CS–, in which the angry face not paired with noise (CS–) was the target and a neutral face was the mask; (iv) seen CS–, in which the CS– angry face was the (perceived) mask and a neutral face was the target. Immediately before the first conditioning sequence, subjects were shown the two angry faces and instructed to press a response button with the index finger of the right hand for each stimulus presentation if they were aware of either angry face. If subjects were not aware of a target angry face they pressed another button with the middle finger of the right hand. Throughout the experiment, subjects' skin conductance responses were monitored to index autonomic conditioning. Details of the acquisition and analysis of the skin conductance response data have been described (9).

RESULTS

Behavioral Tests. None of the masked but all of the unmasked CS+ presentations were detected by subjects. Although they did not exhibit any awareness of the masked faces, subjects had significantly greater skin conductance responses to the unseen CS+ than the unseen CS– faces. These results have been reported in detail (9).

Conditioning Effects. We describe the conditioning effects (i.e., contrasts of CS+ vs. CS– conditions) to provide a background for the regression analysis. Significant responses to CS+ faces were measured bilaterally in the amygdala.

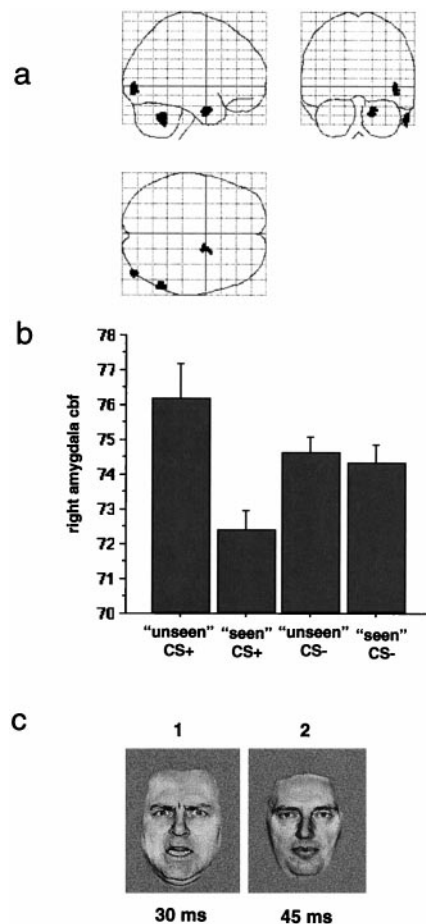


FIG. 1. (a) A statistical parametric map (SPM) showing brain regions significant in the contrast masked CS+ with masked CS– conditions. A threshold of $P < 0.01$ was used for the contrast, and the significant regions are displayed in orthogonal views of a transparent standardized brain image. The activated region in the medial temporal lobe lies within the inferomedial boundary of the right amygdaloid complex. (b) A graphical display of the adjusted regional cerebral blood flow (CBF) in $\text{ml/dl}\cdot\text{min}^{-1}$ at the maximally activated voxel in the right amygdala ($x = 18, y = -2, z = -28$). Bars represent 2 standard errors. (c) A representation of the masked CS+ stimulus condition. An angry face (1), previously paired with a 100-dB noise, is presented for 30 ms and immediately followed by a neutral face (2), never paired with the noise, for 45 ms. The masked angry face (1) is not reported by subjects.

Whereas the right amygdala responded only to the masked CS+ face, the left amygdala showed a differential response only to the unmasked CS+ face (Table 1). Conditioning-related effects also were observed in the cerebellum and regions of extrastriate cortex (Table 1). The conditioning-related amygdala responses (Table 1) have been described in a separate report (9). Responses in all other regions have not been previously reported.

Masking Effects. In the comparison of unmasked (seen) CS+ and masked (unseen) CS+ conditions, a region of the right fusiform gyrus was more active during unmasked presentations (Fig. 2; Table 1). The right globus pallidus and right inferior occipital gyrus, on the other hand, had greater responses in the masked CS+ condition. In the contrast of unmasked and masked CS– faces, an area of cortex in the right temporal pole was more active during unmasked presentations, whereas a medullary region of the brainstem had an enhanced response to masked CS– faces.

Amygdala Connectivity During Masked CS+ Faces. In agreement with our *a priori* prediction, regions of the pulvinar (Fig. 3) and superior colliculus (Fig. 4) covaried positively with

Table 1. Brain region activation caused by conditioning effects

Effect	Contrast	Region	Coordinates,	Z score	P value
			<i>x, y, z</i>		
Conditioning	masked CS+ minus masked CS-	Right amygdala	18, -2, -28	3.42	0.01*
		Right cerebellum	58, -54, -34	3.53	<0.001
		Right inferior occipital gyrus	44, -86, -2	3.45	<0.001
	unmasked CS+ minus unmasked CS-	Left amygdala	-16, -8, -14	2.92	0.02*
		Right lingual gyrus	14, -52, 4	3.73	<0.001
		Right cerebellum	16, -76, -26	3.35	<0.001
Masking	unmasked CS+ minus masked CS+ masked CS+ minus unmasked CS+	Right fusiform gyrus	44, -38, -14	3.97	<0.001
		Right globus pallidus	22, -8, 4	3.43	<0.001
		Right inferior occipital gyrus	50, -82, -10	3.25	<0.001
	unmasked CS- minus masked CS- masked CS- minus unmasked CS-	Right temporal pole	36, 8, -34	3.22	<0.001
		Brainstem (medulla)	0, -38, -42	3.03	0.001

Brain regions showing significant activations as a result of conditioning effects, i.e., comparing CS+ and CS- conditions and masking effects (i.e., comparing masked and unmasked). Coordinates, Z scores and P values are shown for the maximally activated voxels in each contrast. P values for activations in the amygdala are corrected (*) for the volume of brain analyzed, specified as a sphere with radius 8 mm (20).

the right amygdala during masked presentations of the CS+ faces (Table 2). This covariation was specific to the masked CS+ condition: presentation of unmasked CS+ faces did not produce a positive covariation of activity between these structures (Figs. 3*b* and 4*b*). Other regions significant in this analysis included left hippocampus and right extrastriate cortex. By contrast, bilateral regions of orbitofrontal and fusiform cortex showed a negative covariation with the right amygdala specific to the masked CS+ condition (Table 2). A similar regression analysis was performed by using activity in the left amygdala (maximal voxel $x = -16, y = -8, z = -14$) as the covariate of interest. The left amygdala, which responded differentially to seen, but not unseen, target stimuli, covaried positively with bilateral extrastriate cortex (BA18, 19) and right cerebellum but showed no context-specific covariation with pulvinar or superior colliculus.

Amygdala Connectivity During Unmasked CS+ Faces. During presentation of unmasked CS+ faces, the right amygdala demonstrated positive covariation with the right cerebellum, right hippocampus, and bilateral parietal regions (Table 2). In

a similar analysis, the left amygdala covaried positively with the right cerebellum and a left superior parietal region. We had not made any prior predictions about which brain regions would covary with either the right or left amygdala during the unmasked CS+ condition, and none of the identified areas survive correction for multiple comparisons. We report these results, therefore, solely for a descriptive comparison to the pattern of covariation obtained with the masked CS+ condition.

DISCUSSION

These results provide support for the hypothesis that behaviorally relevant features in the visual environment can be detected and processed without conscious awareness by a colliculo-pulvinar-amygdala pathway that also controls reflexive and autonomic responses (Table 2; Figs. 3 and 4). Conscious visual perception (explicit detection) of the same stimuli appears to involve specialized cortical areas e.g., fusiform gyrus and temporal pole (Table 1). Processing by these cortical regions is presumably associated with detailed analysis of the visual scene leading to object categorization and engagement of language processes. The backward masking employed in this study appears to disrupt these cortical processes, while leaving the subcortical tectothalamo-amygdala pathway relatively unaffected (Fig. 2). These findings accord with animal electrophysiological data, discussed below, concerning masking and neural responses in the colliculo-pulvinar pathway.

Single unit recording in monkeys has shown that transient responses in V1, normally occurring immediately after the offset of a target stimulus, are inhibited by masks that render the target invisible to human subjects (28). These transient V1 after-discharges appear to be a critical component of neural processes associated with conscious perception. The disruption of these responses by visual backward masking may provide, therefore, a temporary functional equivalent of the permanent loss of visual awareness seen with striate cortex lesions. Psychophysical experiments have indeed demonstrated blindsight-like effects in healthy subjects by using visual backward-masking techniques (29).

Neural responses of face-selective cells in monkey temporal cortex have been shown to decrease in duration from 200–300 ms to 20–30 ms after backward masking that interferes with conscious perception of faces in human subjects (30). The right fusiform region identified in the present study (Table 1) corresponds to previously reported face-selective activations (31, 32), and as responses in this region were also inhibited by backward masking (Fig. 2), our findings accord with the monkey electrophysiological data. Our results also show evidence of learning-related modulation of fusiform activity, because responses were enhanced to CS+ faces (relative to

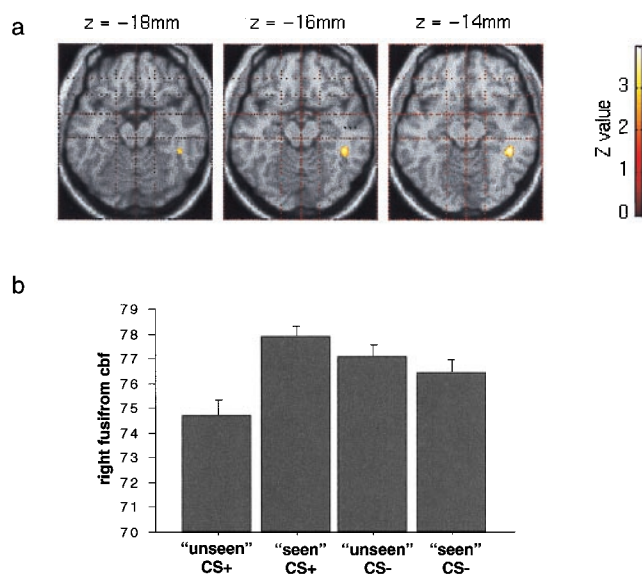


FIG. 2. (a) An SPM showing a region of right fusiform gyrus significantly activated in the contrast of unmasked with masked CS+ conditions. A threshold of $P < 0.01$ was used for the contrast, and the fusiform region is displayed on transverse sections of a canonical structural MRI. (b) A graphical display of the adjusted regional cerebral blood flow (cbf) in $\text{ml/dl}\cdot\text{min}^{-1}$ at the maximally activated voxel in the right fusiform gyrus ($x = 44, y = -38, z = -14$). Bars represent 2 standard errors.

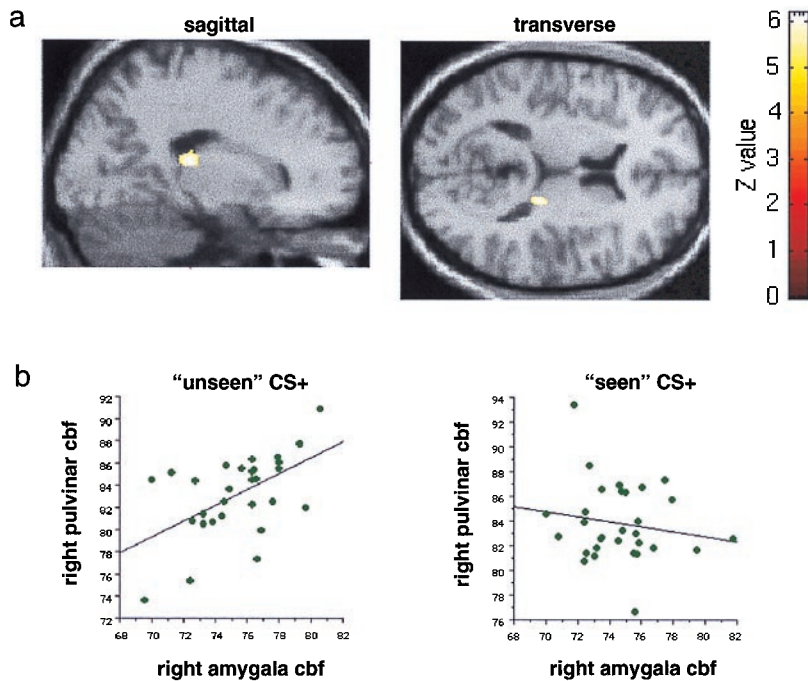


FIG. 3. (a) An SPM showing a region of right pulvinar that exhibits a positive covariation with the right amygdala specifically during presentation of the masked CS+ faces. A corrected threshold of $P < 0.001$ was used for the contrast, which compares the regression slope in the masked CS+ condition with regression slopes in the other three conditions. The region of covariation in the pulvinar is displayed on transverse and sagittal sections of a canonical structural MRI centred on the maximal voxel in the right pulvinar ($x = 18, y = -28, z = 12$). (b) Graphical displays showing bivariate regression plots of right amygdala and right pulvinar activity. The graph on the left plots right amygdala CBF (in $\text{ml/dl}\cdot\text{min}^{-1}$) in the maximal right amygdala voxel ($x = 18, y = -2, z = -28$) and maximal right pulvinar voxel ($x = 18, y = -28, z = 12$) during presentation of the masked CS+ faces. The graph on the right plots right amygdala CBF values for the same voxels in the unmasked condition. Regression lines have been fitted to the data.

CS-), although only when unmasked, i.e., consciously perceived (Fig. 2).

Visual input to the superior colliculus derives from retinal ganglion cells with large, rapidly conducting axons and transient, non-wavelength-sensitive responses (33). Wavelength-sensitive retinal cells with smaller, slower axons and sustained responses are the major source of inputs to the lateral geniculate nucleus (and thus striate cortex) but do not send any projections to superior colliculus (33). Superior colliculus cells respond to flashing or moving stimuli (34), forming a retinotopic map of visual space that assists in guiding saccadic eye movements (35, 36). The rapid, transient responses of collicular cells are well suited to processing briefly presented visual stimuli and so are less vulnerable to backward masking than the sustained responses of geniculostriate cells. Collicular lesions in animals produce deficits in orienting responses (37), responsiveness to novel stimuli (38), and movement discrimination (39). Patients with damage to the colliculi have disturbances in orienting (40) and abnormal modulation of visual-target detection thresholds (18).

The main output projection of the superior colliculus is the posterior thalamic pulvinar nucleus (41), which has direct reciprocal connections with various brain regions, including the amygdala (10). The pulvinar responds selectively to salient visual targets (42), and, like the superior colliculus, is implicated in the control of saccadic eye movements (43, 44). Single unit studies in monkeys have shown that after striate lesions, the colliculo-pulvinar system can still drive activity in dorsal visual areas, such as movement-related MT. However, ventral areas of inferior temporal cortex, specialized for object processing, can only be driven by an intact striate cortex (17). Animal electrophysiological data, therefore, provide strong evidence for functionally distinct, parallel visual pathways that are differentially sensitive to backward masking.

Our data show that several other brain regions, in addition to the predicted structures of the "secondary" visual pathway, covaried in a condition-specific way with the right amygdala. Left posterior hippocampus and right inferior occipital gyrus both had a positive covariation with the amygdala specific to the masked CS+ condition (Table 2). Hippocampus and extrastriate cortex are known to receive strong projections from the amygdala (10), and it has been proposed that these connections are modulatory in nature (45). Evidence for this

view comes from animal studies showing that hippocampal responses are modulated by pharmacological stimulation of the amygdala (46) and from human neuroimaging data revealing significant interactions between amygdala and posterior extrastriate cortex activity during the presentation of emotionally expressive faces (47). The condition-specific covariation between right amygdala, hippocampus, and extrastriate cortex

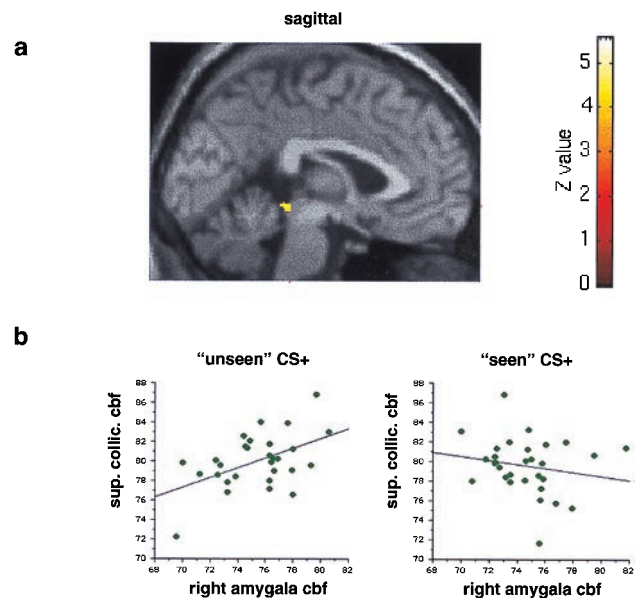


FIG. 4. (a) An SPM showing a region in the superior colliculus that exhibits a positive covariation with the right amygdala specifically during presentation of the masked CS+ faces. The same analysis and threshold was used as in Fig. 3a. The region of covariation in the superior colliculus is displayed on a sagittal section ($y = 0$) of a canonical structural MRI. (b) Graphical displays showing bivariate regression plots of activity in right amygdala and superior colliculus. The graph on the left plots right amygdala CBF (in $\text{ml/dl}\cdot\text{min}^{-1}$) in the maximal right amygdala voxel ($x = 18, y = -2, z = -28$) and maximal collicular voxel ($x = 0, y = -36, z = -8$) during presentation of the masked ("unseen") CS+ faces. The graph on the right plots right amygdala CBF values for the same voxels in the unmasked condition. Regression lines have been fitted to the data.

Table 2. Covariation of brain region with right amygdala

Stimulus category	Regression analysis	Region	Coordinates (x, y, z)	Z score	P value	
Masked CS+	Positive	Left hippocampus	-32, -44, -2	6.31	<0.001*	
			-26, -34, -2	5.66	<0.001*	
		Right pulvinar	18, -28, 12	6.21	<0.001*	
		Left pulvinar (and left medial geniculate)	-22, -24, 0	5.88	<0.001*	
		Right inferior occipital gyrus	54, -70, -2	5.17	<0.01*	
		Superior colliculus	0, -36, -8	4.78	<0.05*	
		Right orbitofrontal cortex	26, 26, -30	6.43	<0.001*	
	Negative	Left orbitofrontal cortex	-38, 14, -16	6.21	<0.001*	
		Right cerebellum	28, -90, -30	5.04	<0.01*	
		Left fusiform gyrus	-42, -48, -26	4.93	<0.05*	
		Brainstem (pons/medulla)	-4, -30, -48	4.12	<0.001	
		Right fusiform gyrus	46, -38, -16	3.28	<0.001	
		Right cerebellum	2, -68, -34	4.16	<0.001	
		Left sup. parietal lobule	-20, -70, 50	3.64	<0.001	
Unmasked CS+	Positive	Right hippocampal gyrus	18, -38, -14	3.56	<0.001	
		Right precuneus	2, -66, 20	3.40	<0.001	
		Left posterior cingulate	-12, -26, 40	3.86	<0.001	
		Ventral midbrain	-10, -38, -16	3.74	<0.001	
		Left amygdala	-16, 4, -22	3.08	0.001	
	Negative					

Brain regions showing a specific positive or negative covariation with the right amygdala (at maximal voxel $x = 18, y = -2, z = -28$) during presentation of masked or unmasked CS+ faces. The regression slope for the condition of interest (i.e., masked or unmasked CS+) was contrasted with the regression slopes in the other three conditions at every voxel in the brain. Coordinates, Z scores, and P values are shown for the maximally activated voxels in each contrast. P values corrected for multiple comparisons are denoted by *.

identified in the present study is consistent, therefore, with the proposed modulatory role for the amygdala.

Bilateral orbitofrontal cortex covaried negatively with right amygdala during presentation of masked CS+ faces (Table 2). Orbitofrontal cortex appears to be important in predicting expected outcomes and adapting responses to different behavioral contingencies (48). Lesions to this region of the brain result in emotional disturbance and a failure to correct inappropriate behavior (48). Orbitofrontal cortex has strong interconnections with the amygdala (10), and it has been proposed that these structures form a crucial circuit in processing behaviorally relevant stimuli (49). The condition-specific change in covariation between right amygdala and orbitofrontal cortex observed in the present analysis is consistent with this conjecture. A masking-sensitive region in right fusiform gyrus also showed negative covariation with the amygdala specific to the masked CS+ condition (Fig. 2; Tables 1 and 2). This relationship between fusiform and amygdala activity may reflect the differential effect of masking on the putative parallel pathways, i.e., retinocolliculo-pulvinar-amygdala and retinogeniculostriate-extrastriate-fusiform.

The subcortical pathway implicated in the processing of masked stimuli by the present data has striking parallels with animal models of fear conditioning (50, 51). Selective lesion experiments have demonstrated a pathway for the rapid processing of conditioned auditory stimuli that involves midbrain inferior colliculus, thalamic medial geniculate nucleus (MGN), and a direct MGN projection to lateral amygdala (50, 51). Amygdala and MGN involvement in auditory fear conditioning has also been demonstrated in a human functional imaging experiment (52). The analogous tectothalamoamygdala pathway identified in the present study also appears to be able to mediate simple autonomic responses to aversively conditioned visual stimuli, whereas explicit or conscious detection of the same stimuli is associated with cortical activation. Our data, therefore, provide evidence for parallel visual pathways in the human brain associated with different levels of conscious awareness. Although subcortical sensory pathways appear sufficient for rapid and unconscious processing of behaviorally important stimuli, the engagement of specialized neocortical areas seems to be required for high-level processes, including object identification and conscious perception.

J.S.M. and R.J.D. are supported by the Wellcome Trust.

- Esteves, F., Dimberg, U. & Öhman, A. (1994) *Cognit. Emotion* **8**, 393–413.
- Bechara, A., Tranel, D., Damasio, H., Adolphs, R., Rockland, C. & Damasio, A. R. (1995) *Science* **269**, 1115–1118.
- LaBar, K. S., LeDoux, J. E., Spencer, D. D. & Phelps, E. A. (1995) *J. Neurosci.* **15**, 6846–6855.
- Adolphs, R., Tranel, D., Damasio, H. & Damasio, A. R. (1994) *Nature (London)* **372**, 669–672.
- Calder, A. J., Young, A. W., Rowland, D., Perrett, D. I., Hodges, J. R. & Etcoff, N. L. (1996) *Cogn. Neuropsychol.* **13**, 699–745.
- Breiter, H. C., Etcoff, N. L., Whalen, P. J., Kennedy, D. N., Rauch, S. L., Buckner, R. L., Strauss, M. M., Hyman, S. E. & Rosen, B. R. (1996) *Neuron* **2**, 875–887.
- Morris, J. S., Frith, C. D., Perrett, D. I., Rowland, D., Young, A. W., Calder, A. J. & Dolan, R. J. (1996) *Nature (London)* **383**, 812–815.
- Whalen, P. J., Rauch, S. L., Etcoff, N. L., McNerney, S. C., Lee, M. B. & Jenike, M. A. (1998) *J. Neurosci.* **18**, 411–418.
- Morris, J. S., Öhman, A. & Dolan, R. J. (1998) *Nature (London)* **393**, 467–470.
- Amaral, D. G., Price, J. L., Pitkanen, A. & Carmichael, S. T. (1992) in *The Amygdala: Neurobiological Aspects of Emotion, Memory and Mental Dysfunction*, ed. Aggleton, J. P. (Wiley-Liss, New York), pp. 1–66.
- Weiskrantz, L., Warrington, E. K., Sanders, M. D. & Marshall, J. (1974) *Brain* **97**, 709–728.
- Barbur, J. L., Ruddock, K. H. & Waterfield, V. A. (1980) *Brain* **103**, 905–928.
- Blythe, I. M., Kennard, C. & Ruddock, K. H. (1987) *Brain* **110**, 887–905.
- Weiskrantz, L., Barbur, J. L. & Sahraie, A. (1995) *Proc. Natl. Acad. Sci. USA* **92**, 6122–6126.
- Schneider, G. E. (1969) *Science* **163**, 895–902.
- Zihl, J. & von Cramon, D. (1979) *Brain* **102**, 835–856.
- Gross, C. G. (1991) *Neuropsychologia* **29**, 497–515.
- Zihl, J. & von Cramon, D. (1979) *Exp. Brain Res.* **35**, 419–424.
- Ptito, A., Lepore, F., Ptito, M. & Lassonde, M. (1991) *Brain* **114**, 497–512.
- Ptito, M., Johannsen, P., Danielsen, E., Faubert, J., Dalby, M. & Gjedde, A. (1997) *Neuroimage* **5**, Suppl., S145.
- Sahraie, A., Weiskrantz, L., Barbur, J. L., Simmons, A., Williams, S. C. R. & Brammer, M. J. (1997) *Proc. Natl. Acad. Sci. USA* **94**, 9406–9411.

22. Tomaiuolo, F., Ptito, M., Marzi, C. A., Paus, T. & Ptito, A. (1997) *Brain* **120**, 795–803.
23. Jones, E. G. & Burton, H. (1976) *Brain Res.* **104**, 142–147.
24. Friston, K. J., Buechal, C., Fink, G., Morris, J. S., Rolls, E. T. & Dolan, R. J. (1997) *Neuroimage* **6**, 218–229.
25. Friston, K. J., Holmes, A. P., Worsley, K. J., Poline, J.-P., Frith, C. D. & Frackowiak, R. S. J. (1995) *Hum. Brain Mapp.* **2**, 189–210.
26. Friston, K. J., Ashburner, J., Poline, J.-P., Frith, C. D. & Frackowiak, R. S. J. (1995) *Hum. Brain Mapp.* **3**, 165–189.
27. Worsley, K. J., Marrett, P., Neelin, A. C., Friston, K. J. & Evans, A. C. (1996) *Hum. Brain Mapp.* **4**, 58–73.
28. Macknik, S. L. & Livingstone, M. S. (1998) *Nat. Neurosci.* **1**, 144–149.
29. Meeres, S. L. & Graves, R. E. (1990) *Neuropsychologia* **28**, 1231–1237.
30. Rolls, E. T. & Tovee, M. J. (1994) *Proc. R. Soc. London Ser. B* **257**, 9–15.
31. Haxby, J. V., Horwitz, B., Ungerleider, L. G., Maisog, J. M., Pietrini, P. & Grady, C. L. (1994) *J. Neurosci.* **14**, 6336–6353.
32. Dolan, R. J., Fink, G. R., Rolls, E., Booth, M., Holmes, A., Frackowiak, R. S. J. & Friston, K. J. (1997) *Nature (London)* **398**, 596–599.
33. Schiller, P. H. & Malpeli, J. G. (1977) *J. Neurophysiol.* **40**, 428–445.
34. Moors, J. & Vendrik, A. J. (1979) *Exp. Brain Res.* **35**, 333–347.
35. Wurtz, R. H. & Goldberg, M. E. (1971) *Science* **171**, 82–84.
36. Robinson, D. (1972) *Vision Res.* **12**, 1795–1808.
37. Goodale, M. A. & Murison, R. C. (1975) *Brain Res.* **88**, 243–261.
38. Milner, A. D., Foreman, N. P. & Goodale, M. A. (1978) *Neuropsychologia* **16**, 381–390.
39. Collin, N. G. & Cowey, A. (1980) *Exp. Brain Res.* **35**, 419–424.
40. Rafal, R. D., Posner, M. I., Friedman, J. H., Inhoff, A. W. & Bernstein, E. (1988) *Brain* **111**, 267–280.
41. Bevenuto, L. A. & Fallon, J. H. (1975) *J. Comp. Neurol.* **160**, 339–362.
42. Morris, J. S., Friston, K. J. & Dolan, R. J. (1997) *Proc. R. Soc. London Ser. B* **264**, 760–775.
43. Petersen, S. E., Robinson, D. L. & Keys, W. (1985) *J. Neurophysiol.* **54**, 867–886.
44. Petersen, S. E., Robinson, D. L. & Morris, J. D. (1987) *Neuropsychologia* **25**, 97–105.
45. Cahill, L. & McGaugh, J. L. (1998) *Trends Neurosci.* **21**, 294–299.
46. McGaugh, J. L., Intorini-Collisin, I. B., Cahill, L., Kim, M. & Liang, K. C. (1992) in *The Amygdala: Neurobiological Aspects of Emotion, Memory and Mental Dysfunction*, ed. Aggleton, J. P. (Wiley-Liss, New York), pp. 143–167.
47. Morris, J. S., Friston, K. J., Buechal, C., Frith, C. D., Young, A. W., Calder, A. J. & Dolan, R. J. (1998) *Brain* **121**, 47–57.
48. Rolls, E. T. (1995) in *The Cognitive Neurosciences*, ed. Gazzaniga, M. S. (MIT Press, Cambridge, MA), pp. 1091–1106.
49. Schoenbaum, G., Chiba, A. A. & Gallagher, M. (1998) *Nat. Neurosci.* **1**, 155–159.
50. LeDoux, J. E. (1995) in *The Cognitive Neurosciences*, ed. Gazzaniga, M. S. (MIT Press, Cambridge, MA), pp. 1049–1061.
51. Weinberger, N. M. (1995) in *The Cognitive Neurosciences*, ed. Gazzaniga, M. S. (MIT Press, Cambridge, MA), pp. 1071–1089.
52. Morris, J. S., Friston, K. J. & Dolan, R. J. (1998) *Proc. R. Soc. London Ser. B* **265**, 649–657.